Potential Effects of Climate Change on Black Sea Water Temperatures

Ufuk OZKAN[a,*], Bilge TUTAK[b,*]

aIstanbul Technical University, Eurasia Institute of Earth Sciences, Istanbul, Turkey

bIstanbul Technical University, Faculty of Naval Architecture and Ocean Engineering, Istanbul, Turkey

ORCIDs:

Ufuk OZKAN: 0000-0002-9862-4334

Bilge TUTAK: 0000-0003-2885-9338

* Corresponding Authors: ozkan15@itu.edu.tr, tutak@itu.edu.tr

This is a non-peer reviewed preprint submitted to EarthArxiv.

Abstract

There is a consensus that the Black Sea is affected by climate change in many ways. The Black Sea Physical Reanalysis system and Argo measurements are used for analyzing not only sea surface temperature (SST), but also the entire Black Sea over the period from 1993 to 2019. Linear regression and Mann-Kendall tests are used for detecting trends and the Pearson-correlation coefficient is used for detecting correlation between data sets. Results show that the entire Black Sea has been warming with few abrupt exceptions such as in 2012 and 2017. In addition, water masses in the upper water column have been warming (CIL = 0.012 °C/year, BSSW (Black Sea Surface Water) and BSCW (Black Sea Coastal Water) = 0.096 °C/year). However, there is no statistically significant trend in deeper parts of the Black Sea. The western shelf, especially its west coasts, is the region that is most open to seasonal changes in the Black Sea.

Keywords: Black Sea, Climate Change, Copernicus, Argo, Temperature, Warming

1. **Introduction**

Climate change has been researched many times for many years. Researchers point out climate warming all over the world because of the industrial revolution (Esser et al., 2011; Bernstein et al., 2008). Predictions show that warming will not stop until the end of the 21st century. According to the Intergovernmental Panel of Climate Change(IPCC), the impacts and risks of climate change are getting significantly dangerous as the emission of greenhouse gases has been increasing intensively. Marine ecosystems changed with the impacts of climate change more than expected (Rhein et al., 2013; Clark et al., 2016; IPCC, 2014). There are many researches about the impacts of climate change at both global and regional scales (Stanev and Peneva, 2001; Sakalli and Basusta, 2018; Jones, 2001; Patz et al., 2005). As Mee et al. (2005) stated, marine habitats have been changing on the shelves of the Black Sea since the seventies. In addition, sea surface temperature (SST) has been the subject of many studies (Shapiro et al., 2010; Kazmin and Zatsepin, 2007; Sakalli and Basusta, 2018; Ginzburg et al., 2004). Although there are cooling and warming events, Black Sea SST increased in the last century(Oguz et al.,2006). Furthermore, more than half of the Marine Heatwaves occurred in the last century in the Black Sea(Mohamed et al.,2022). Cold Intermediate Layer (CIL) has been changing (Miladinova et al., 2018) and there is a probability that CIL may disappear in the future (Stanev et al., 2019). However, there is a few information about Black Sea Water Masses other than SST and CIL. In addition to this, due to climate change, water masses in the Black Sea are also changing and might require new definitions. Information about the changes in physical properties in different water masses (Table 1) is a key to understand the changes in the ecosystem of the Black Sea.The Black Sea is separated from the other seas and oceans by having unique properties such as Rim Current, positive freshwater balance, etc. Azov Sea and Mediterranean Sea (through Turkish Strait System) are the only seas having water exchange with the Black Sea. In addition, salinity in the Black Sea is governed by deep Mediterranean water and evaporation. As a result, there is strong density stratification, and compared to the other oceans vertical mixing of Black Sea is relatively weak. Because of the stratified structure of the Black Sea, the water column under 100 m depth is generally anoxic (Stewart et al., 2007). Weak vertical mixing causes the formation of a unique water mass that is called the Cold Intermediate Layer. CIL forms between warm surface water (25 °C) and relatively warm deep water (9 °C). CIL is characterized by being lower than 8 °C (Ozsoy and Unluata, 1997). Furthermore, the bottom topography of the Black Sea can be

58 characterized by three basic forms. One of them is shelf areas, which are shallow ($< 200\ m$).
59 The second one is the abyssal plain, which is the deep part of the Black Sea($> 2000\ m$) and
60 there is a steep continental slope between shelf areas and the deep abyssal plain.

61 Other than CIL and SST changes, our approach is to investigate the different water masses in the
62 Black Sea (Table 1) from 1993 to 2019. Through this methodology the identification of changes
63 for the entire basin is possible. First, the temporal analysis will be applied to the entire Black Sea
64 water body. Later, the same temporal analysis is applied to the different water masses in the
65 Black Sea that are commonly used in literature (Ivanov and Belokopytov, 2013). Finally, spatial
66 analysis is used for the entire basin and to the surface for both seasonal and annual variations.

67 The structure of the paper is as follows: After the literature, in the second part the data sets and
68 the methods, which are used for finding trends, are described. In the third section, we present the
69 results which are followed by a discussion of the results in section four.

2. Materials and Methods

2.1. Study Area and Data

72 The water input of the Black Sea can be divided into two categories. On one hand, there is fresh
73 water input which is driven by river runoff and precipitation. On the other hand, there is warmer
74 and more saline water which is coming from the Mediterranean Sea and the evaporation at the
75 surface. Differences in water inputs lead to a strong stratification in water masses. Thus, Different
76 water masses in the Black Sea are investigated. Determination of the water masses is decided
77 using Glazkov's definitions (Ivanov and Belokopytov, 2013) for the identification of water
78 masses (Table 1).

83 Table.1 : Identification of water masses of Black Sea. BSCW is Black Sea Coastal Water. BSSW

84 is Black Sea Surface Water. CIL is Cold Intermediate Layer. BSIW is Black Sea Intermediate

85 Water and BSDW is Black Sea Deep Water (taken from Ivanov and Belokopytov, 2013).

Water mass	Glazkov, 1979	Gertman,1991	Mamayev et al, 1994	Belokopytov, 2004
BSCW	S<17 (0.2%)	S<17 (0.05%)	T>8 S<20 (3.5%)	S<=17.8 (0.5%)
BSSW	S=17.4-18.6 (4.2%)	S=17.4-18.6 (3.8%)		S=18.0-18.4 σ<14.0 (2.3%)
CIL	T≤8 (2.9%)	S=18.6-20 (3.7%)	T≤8 (4.5%)	T=6.0-7.8 S=18.0-19.0 σ =14.0-14.8 (2.2%)
BSIW	T=8-9 S=21.6-22.2 (50.2%)	S=20-22.2 (43.5%)	S>20 (92%)	T=7.8-8.98 S=19.0-22.30 σ =14.8-17.19 (55%)
BSDW	T=8-9 S=22.2-22.4 (45.4%)	S>22.2 (49%)		T=8.98-9.11 S=22.30-2.34 σ =17.19-17.21 (40%)

86

87 Table.2 : Root Mean Square Difference and Bias are calculated over the period 1993 to 2018.

88 Calculations are done between the other Black Sea reanalysis products which are

89 BS_REAN_V01 and BS_REAN_V02. (Table is taken from Lima et al.,2020)

	RMSD		BIAS	
	BS_REAN_V1	BS_REAN_V2	BS_REAN_V1	BS_REAN_V2
SST	0.35	0.33	0.08	0.08
0-10	1.217	0.593	-0.45	0.006
10-100	1.274	0.634	0.051	-0.031
100-500	0.131	0.072	0.039	0.001
500-1500	0.099	0.066	0.092	0.053

90

91   To investigate temperature and salinity changes in the Black Sea, we used the Black Sea Physical

92   Reanalysis system data (monthly, 1/27° × 1/36° km resolutions) from E.U. Copernicus Marine

93   Services over the period January 1993 to December 2019 (Lima et al., 2020). The base of the

94   model's hydrodynamical core is NEMO general circulation ocean model. ECMWF ERA5

95   computes atmospheric surface fluxes, which force NEMO, by bulk formulation. The resolution of

96   atmospheric fields is 0.25° in space and 1 hour in time. The accuracy of the model is shown in

97   Table 2. Further details can be found on the official the website of

98   model(https://doi.org/10.25423/CMCC/BLKSEA_MULTIYEAR_PHY_007_004). We used

99   monthly mean temperature and salinity distributions for temporal analysis. Then, mean,

100   minimum and maximum values of temperatures and salinity are used for further analyzing the

101   temporal distributions annually. The monthly temporal distribution of different water masses

102   (Table 1) is investigated. Moreover, the spatial distribution of data is shown in two ways. The

103   first one is depth-averaged data which is analyzed both seasonally and annually. The second one

104   is sea surface temperature (SST) data which is also analyzed both seasonally and annually.

105   Spatial mean values are presented as means ± standard deviation and warm waters are calculated

106   by adding two times of standard deviation to the mean temperature.

107
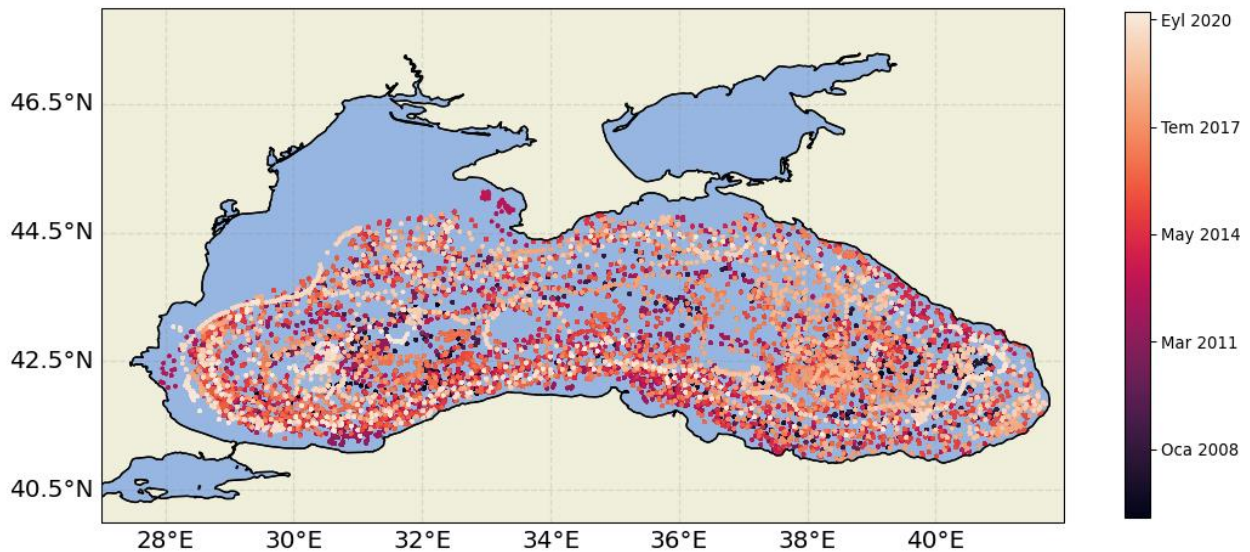
108   Figure 1: Argo Floats trajectories with time.

For validation of reanalysis data, Argo data were used as an in-situ measurement. These data were collected and made freely available by the International Argo Program and the national programs that contribute it (https://argo.ucsd.edu, https://www.ocean-ops.org). The Argo Program is part of the Global Ocean Observing System. The time period of Argo data is ranging from 2005 to 2021. Code numbers, profiling depths, parking depths and amount of cycles of Argo Floats are listed in Table 2 and profiling places are shown in Figure 1. Argo floats collect temperature, salinity and density data from the surface to its profiling pressure and drifts in parking pressure. Accuracies of the data are 0.002 °C in temperature, 2.4 dbar in pressure and 0.01 PSU in salinity after delayed mode adjustments (Wong et al., 2020).

Table.2 : Parking and profiling pressure, the amount of cycle and start/ending data of Argo floats.

Float No	LATITUDE(N)	LONGITUDE(E)	Parking Pressure	Profiling Pressure	Start Date	End Date	Cycle
1901200	42.92	28.88	200	1500	8.12.2009	23.02.2013	234
3901852	42.18	29.33	200	1500	6.12.2016	-	411
3901854	43.58	30.44	200	1500	2.11.2016	-	418
3901855	43.11	28.88	200	1500	22.10.2016	17.06.2022	411
4900489	41.88	29.58	1500	1550	7.03.2005	18.01.2019	195
4900540	41.87	29.57	1500	1550	7.03.2005	2.10.2008	180
4900541	42.13	30.25	1500	1550	12.06.2006	1.03.2009	133
4900542	42.15	30.27	1500	1550	13.06.2006	23.12.2009	174
5902291	41.43	29.51	1300	1300	16.04.2010	17.04.2010	23
6900803	43.34	30.67	750	1500	18.03.2011	18.10.2017	482
6900804	42.73	30.26	750	1500	18.03.2011	1.07.2013	168
6900805	43	29	750	1500	19.03.2011	12.11.2016	414
6900807	43.95	31.35	200	1000	28.11.2014	3.09.2018	259
6901828	42.83	28.82	200	1500	29.09.2013	24.08.2014	66
6901831	43.16	29	200	1500	18.07.2014	21.11.2019	391
6901832	43.16	29	200	1500	12.09.2014	16.03.2020	403
6901833	42.24	39.87	200	1500	1.06.2016	19.03.2021	351
6901834	43.16	28.99	200	1500	25.11.2015	4.04.2021	392
6901866	43.16	29	200	1000	27.05.2015	12.07.2019	302
6901895	42.22	35.28	750	750	2.08.2013	26.01.2017	255
6901896	41.87	29.53	200	750	4.08.2013	5.10.2014	86
6901899	41.62	29.44	500	1000	2.05.2014	10.11.2014	39
6901900	41.54	29.47	200	1000	2.05.2014	22.07.2016	163
6901959	43.47	29.66	200	1500	8.06.2012	21.04.2015	210
6901960	43.17	29.66	200	1500	9.06.2012	11.06.2012	26
6901961	43.15	30.77	200	1500	6.11.2012	19.09.2015	210

Float No	LATITUDE(N)	LONGITUDE(E)	Parking Pressure	Profiling Pressure	Start Date	End Date	Cycle
6901962	43.47	29.66	200	1500	17.08.2012	20.07.2015	214
6903228	43.41	29.52	200	1500	20.10.2017	12.02.2018	24
6903240	43.17	29	1000	1000	29.03.2018	13.07.2022	324
6903271	44.54	30.97	200	1500	1.10.2019	22.07.2022	350
6903766	43.18	29	200	1500	2.12.2019	25.07.2022	194
6903782	43.03	28.75	200	1500	23.07.2020	25.07.2022	148
6903865	42.98	28.23	40	50	24.07.2020	5.08.2020	94
6903866	42.50	28.83	750	1500	22.11.2020	27.07.2022	123
6903867	43.17	29.16	750	1500	17.11.2020	22.07.2022	123
7900465	44.17	32.5	450	500	7.05.2010	7.03.2012	134
7900466	44	32.08	450	500	7.05.2010	27.11.2012	187
7900590	43	29	750	2000	29.08.2013	2.07.2015	135
7900591	43.24	29.24	1000	1000	16.12.2013	20.02.2020	264
7900592	42.24	29	1000	1000	15.12.2013	25.10.2014	79
7900593	43.17	29	750	2000	2.06.2014	15.04.2015	64
7900594	43.17	29	750	2000	26.06.2015	2.06.2017	142
7900595	43.16	29.15	1000	2000	10.08.2019	17.07.2022	108
7900596	42.48	28.64	1000	2000	5.12.2019	24.07.2022	97

119

120 As a validation, we resampled the data as monthly and yearly. Monthly data is used in the
121 temporal distribution of temperature and salinity. Moreover, monthly data are investigated in
122 different water masses. On the other hand, yearly data is used as a minimum, mean and maximum
123 values of both temperature and salinity.

124 **2.2. Statistical Methods**

125 The Mann-Kendal test is a robust test which is used for detecting a trend in time-series data. It is
126 a non-parametric test, which means that it can be used for all distributions. The test calculates S
127 statistics by using Eq.(1)

128 $S = \sum_{k=1}^{n-1}\sum_{j=k+1}^{n} sgn(x_j - x_k)$ (1)

129 where n is the number of data points, $x_j \, and \, x_k$ are annual values and $sgn(x_j - x_k)$ is sign
130 function. Having a positive value of S indicates an increasing trend and vice versa. If the value of
131 S equals to zero there is no trend. Moreover, if n is bigger than 10, the S-statistics approach to

132   normal distribution. The mean value of S equals to zero and the variance of S is calculated by

133   using in Eq.(2)

134     $var(S) = \frac{(n(n-1)(2n+5))-\sum_{i=1}^{n} t_i(t_i-1)(2t_i+5)}{18}$ (2)

135   Where n is the number of tied group(there is no difference between compared values) and t_i is

136   the number of the data values in i^{th} group. Z-statistics is calculated by Eq.(3)

137     $Z = \begin{cases} \frac{S-1}{\sqrt{var(S)}} & if\ S > 0 \\ S = 0 & if\ S = 0 \\ \frac{S+1}{\sqrt{var(S)}} & if\ S < 0 \end{cases}$ (3)

138   Trend assessment is based on a sign of Z value. A positive value of Z indicates a statically

139   significant increasing trend, whereas, negative value of Z indicates a statically significant

140   decreasing trend. The Seasonal Mann-Kendal test(Hirsch and Slack,1984) is used on monthly

141   data for clearing the seasonality effect. We used pyMannKendall library(Hussain et al.,2019) in

142   Python software for applying both Mann-Kendal and seasonal Mann-Kendal tests.

143   We analyzed the linear trend in both temporal and spatial distributions. Simple linear regression

144   used for analysis given in the general form is the following equation;

145     $y = mx + c$ (4)

146   where y is the temperature or the salinity and x is the time in years or months. For finding m and

147   c coefficients following equations are used;

148     $m = \frac{\sum y - b \sum x}{N}$ (5)

149     $c = \frac{N \sum xy - \sum x \cdot \sum y}{N \sum x^2 - (\sum x)^2}$ (6)

150   where N is the number of all temperature or salinity estimations.

151   Pearson-correlation coefficient (r) is used for observation of correlation between Argo data and

152   model data. For calculation of r following equation is used;

153     $r = \frac{\sum(X_i - \bar{X})(Y_i - \bar{Y})}{\sqrt{\sum(X_i - \bar{X})^2 \sum(Y_i - \bar{Y})^2}}$ (7)

154   where X and Y are variables, $\bar{X}\ and\ \bar{Y}$ are the mean of X and Y, respectively. Values of r is

155 ranging from -1 to 1. Pearson-correlation coefficient of 0 means no correlation between Argo
156 measurements and model result. On the other hand, Pearson-correlation coefficient of 1 indicates
157 that variables change in the same direction. Whereas, Pearson-correlation coefficient of -1
158 indicates that variables change in the opposite direction. Details of Pearson-correlation
159 coefficient were given by Benesty et al. (2009).

3. Results

161 The depth averaged monthly mean temperatures are shown in Figure.2. They increase over the
162 period 1993 to 2019 years ($z = 16.47, p = 0$). The increasing trend begins in 1993 and stops
163 over the period 2000 and 2006. Temperatures are oscillating in this period of time. After 2006 the
164 increasing trend continues. Also, Argo measurements indicate that there is an increasing trend
165 over the period 2006 and 2021($z = 7.81, p = 0$). Moreover, Argo and model data highly
166 correlated over the period January 2006 to December 2019 with the Pearson-correlation
167 coefficient of 0.92. On the other hand, there are differences between the model results and Argo
168 data, especially in the first 100 meters in depth where the model can overestimate temperatures
169 (Table 2). Nearly one-third of the Argo measurements are taken in the first 100 meters in depth
170 and another almost one-third of the Argo measurements are taken between 100 and 200 meters in
171 depth(Figure 4). In addition to that, Argo temperatures are in the range of the model's accuracies
172 except over the depths of 500 and 1500 meters(Figure 3). In that depth range, there is a small
173 amount of measurement and after 1000 meters in depth, there is nearly no data. However, in the
174 first 100 meters in depth, the model and Argo measurements follow the same trend. In between
175 100 and 500 meters in depth, Argo measurements and model results are almost the same
176 especially after 2015, when the amount of Argo measurements increased significantly(Figure 4).

Monthly Mean Temperature of Black Sea

y = 0.0032x + 9.033
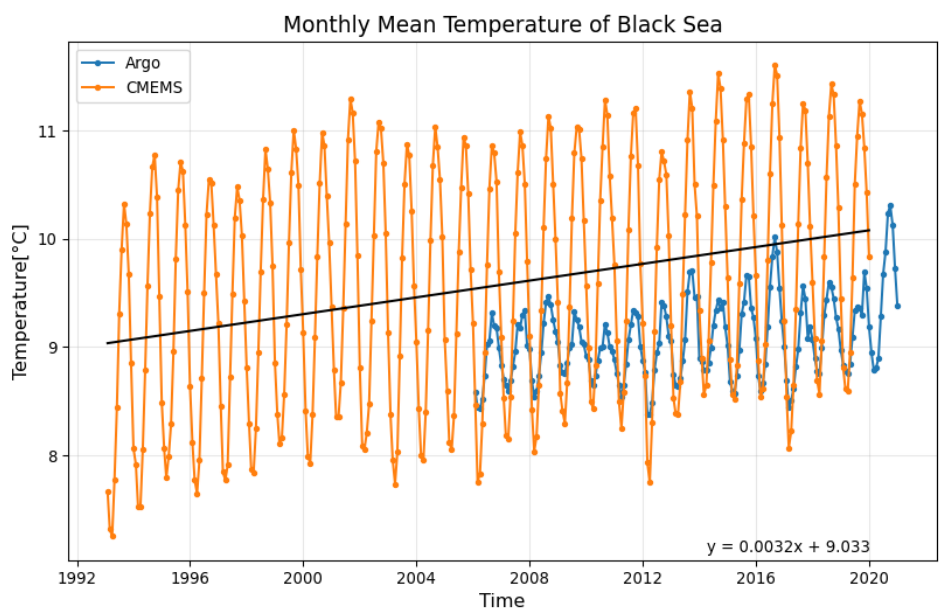
177

178 Figure 2: Depth averaged monthly mean temperaturesover the period January 1993 to 2019.
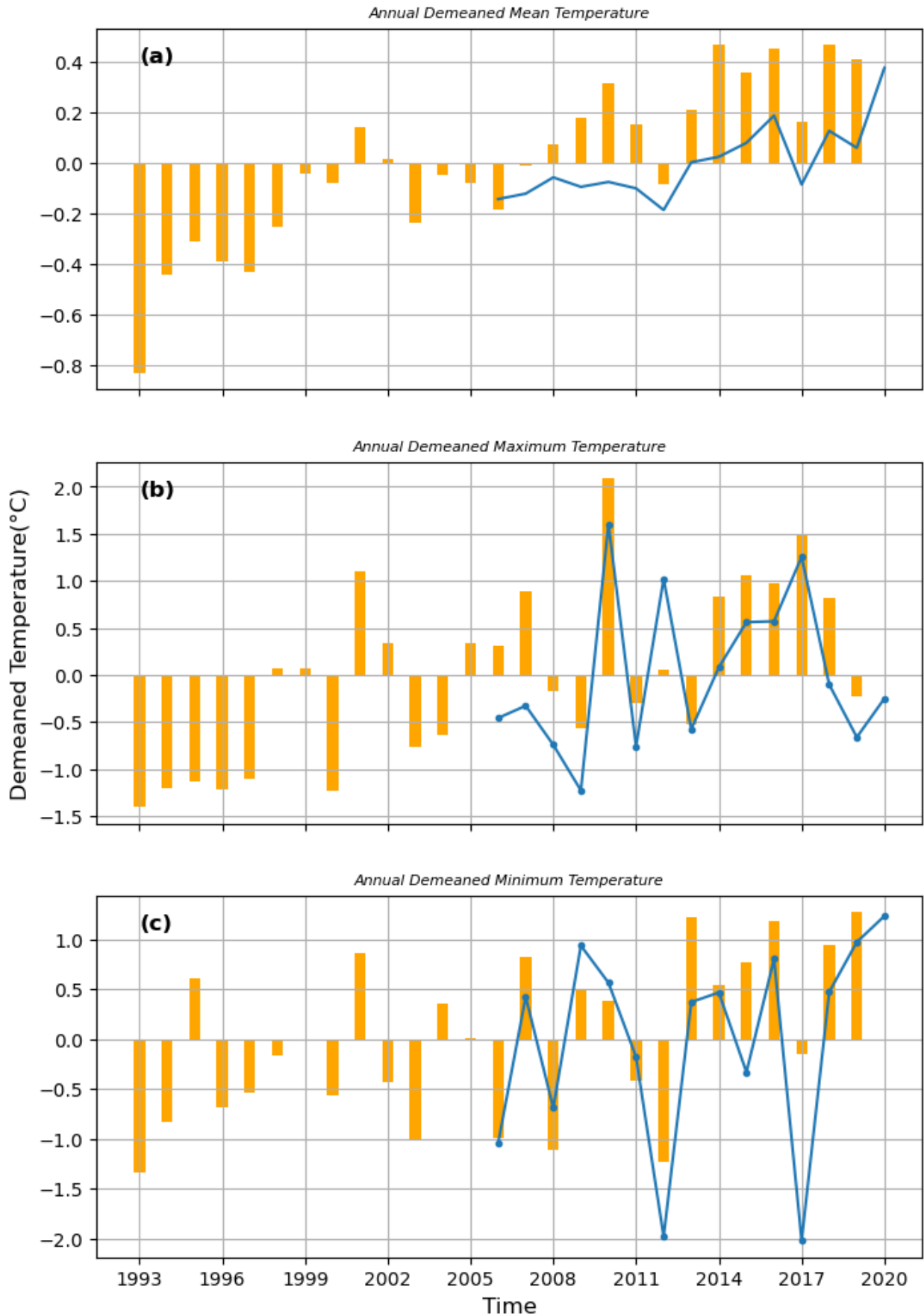179 Black line is the linear trend line, blue line is the Argo data.
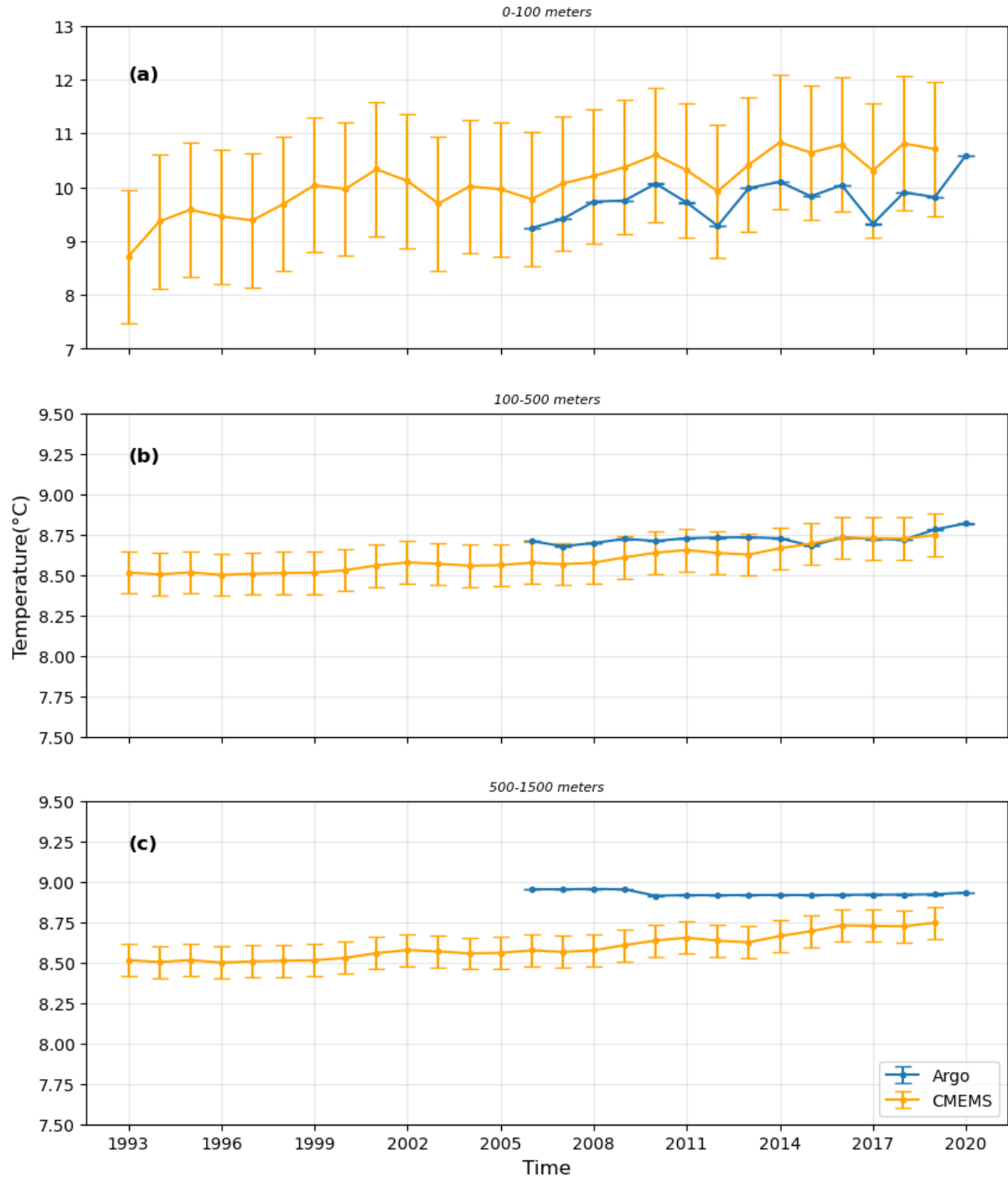
Figure.3: Depth averaged monthly mean temperatures with error bars in between (a) 0 and 100 meters, (b) 100 and 500 meters and (c) 500 and 1500 meters in depth. Error in Argo measurements are 0.002 °C(Wong et al., 2020) and errors in model results are given in Table.2.

184
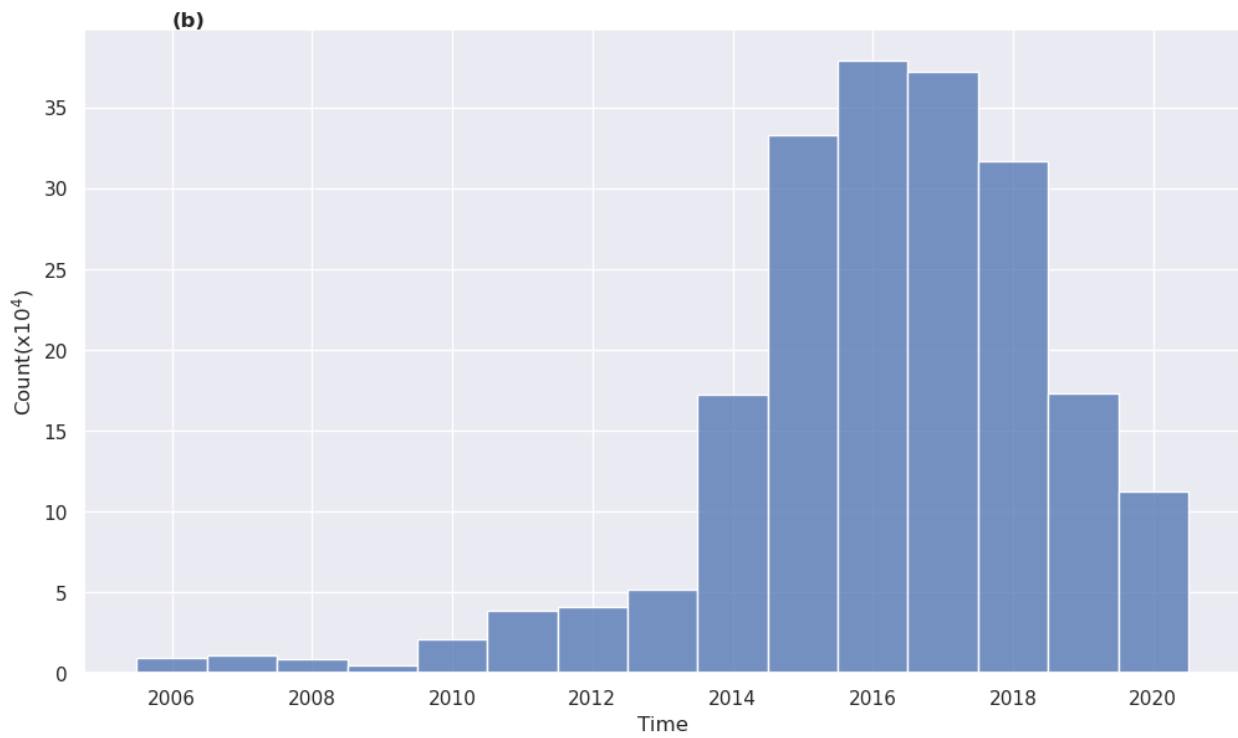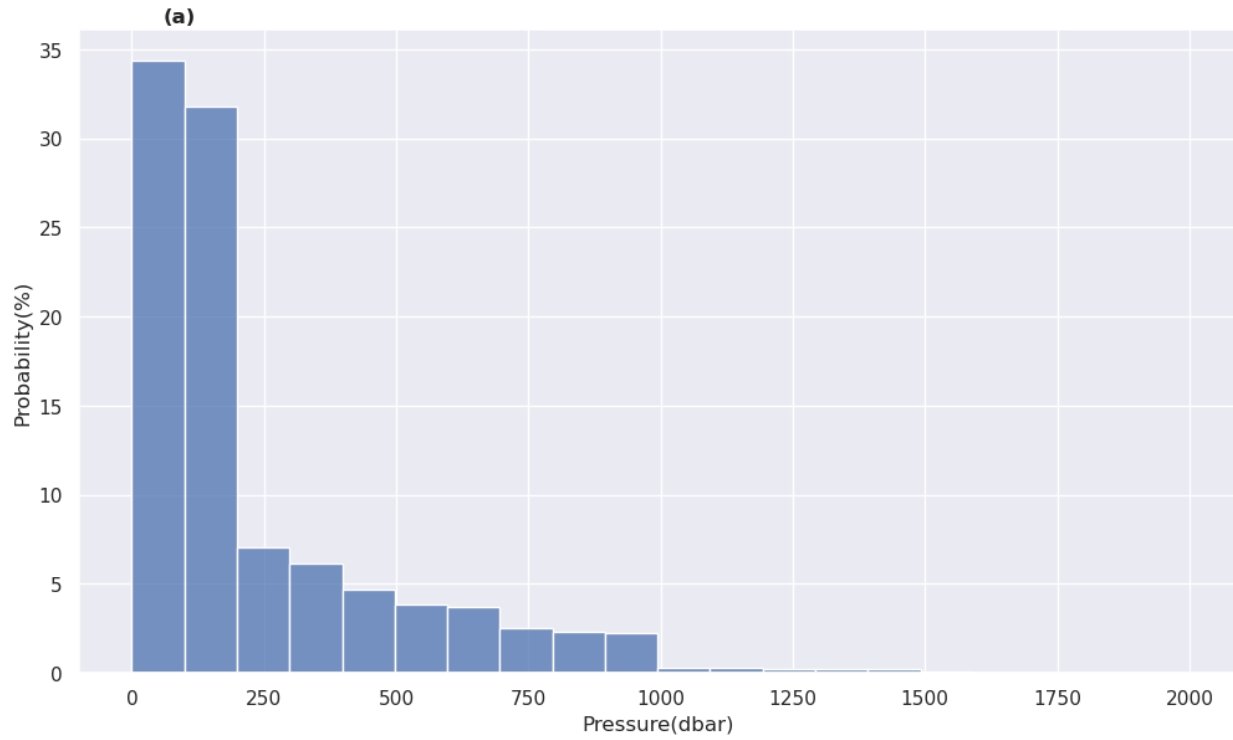
Figure 4: Histogram plot of Argo measurements. Each bins are 100 meters.

Annual Demeaned Mean Temperature

Annual Demeaned Maximum Temperature

Annual Demeaned Minimum Temperature

187   Figure 5: Depth averaged demeaned annual (a) mean, (b) maximum, (c) minimum temperatures

188   for the Black Sea over the period January 1993 to 2020. Orange bars show the demeaned model

189   results and blue line shows demeaned Argo data.

190   Demeaned temperatures of the Black Sea are represented in Figure 5. Depth-averaged mean

191   temperature anomalies are above average after 2007 and they are below average before 2007 with

192   a few exceptions such as in 2012. Overall, an increase trend is detected at demeaned annual mean

193   temperatures $(z = 5.21, p = 0)$. Although there are exceptions in maximum and minimum

194   demeaned temperatures, they also tend to increase $(z_{max} = 3.21, p = 0.001; z_{min} = 2.79, p = $

195     $0.005)$.. On the other handmean temperature decreases in 2012 and 2017 in both model and Argo

196   data. Furthermore, Argo and model data are highly correlated $(r = 0.86)$ over the period 2006 to

197   2019.

198
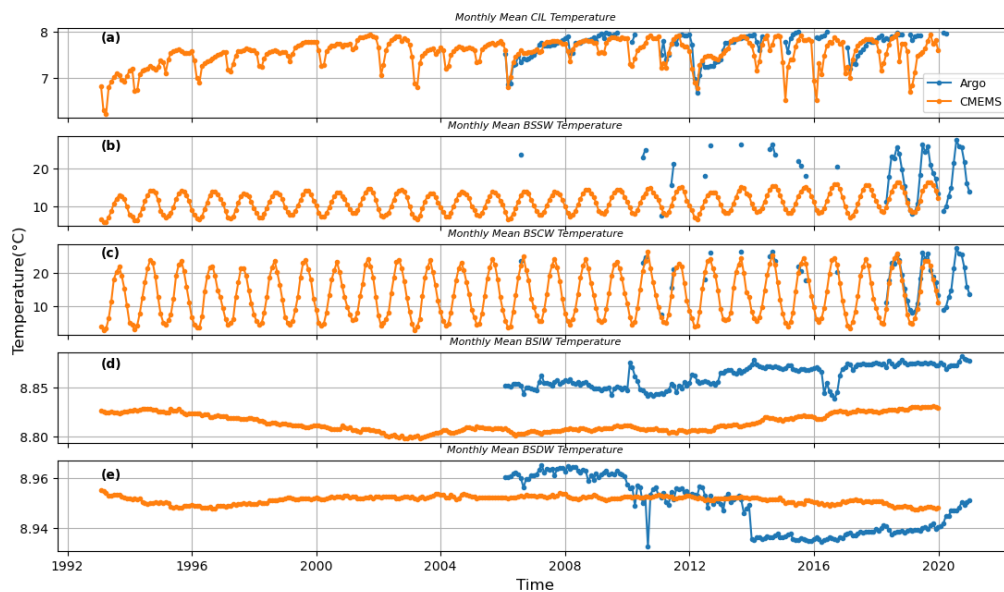
199

200   Figure 6: Depth averaged monthly mean temperatures in different water masses (Table 1) such as

201   (**a**) CIL, (**b**) BSSW, (**c**) BSCW, (**d**) BSIW and (**e**) BSDW. Blue line shows Argo data and orange

202   line shows model data.

203   For a better understanding of the change in temperature characteristics, we analyzed temperatures

204   in different water masses (Table 1) by applying the Seasonal Mann-Kendall test and linear trend

205   detection to model results (Figure 6). CIL is warming at a rate of 0.001 °C per month. The

206   Seasonal Mann-Kendall test indicates this result with the z-statistic value of 6.71 and p-value of
207   0. This increase is highly important since there is a chance that CIL may disappear in the future
208   (Stanev et al., 2019). Moreover, increasing trends are detected from both BSSW ($z = 15.45, p = 0$) and BSCW ($z = 9.56, p = 0$) at a rate of 0.008 °C per month. Although Pearson correlation
210   coefficient can not be determined, because of Argo data having missing values, high correlation
211   in CIL, BSSW and BSCW between Argo measurements and model result can be visibly observed
212   in Figure 6a, 6b and 6c. On the other hand, the correlation between two datasets in terms of
213   BSIW and BSDW is relatively low ($r_{BSIW} = 0.73, r_{BSDW} = 0.69$) over the period January 2006
214   to December 2019 (Figure 6d, Figure 6e). Furthermore, a significant trend is not detected in
215   BSIW ($z = 1.47, p = 0.14$) and decreasing trend is detected in BSDP ($z = -2.50, p = 0.01$).
216   However, the magnitude of the trend is 10^{-6}, hence it is not important as well. This indicates that
217   the change in temperature characteristic of the Black Sea is not present in deep layers.
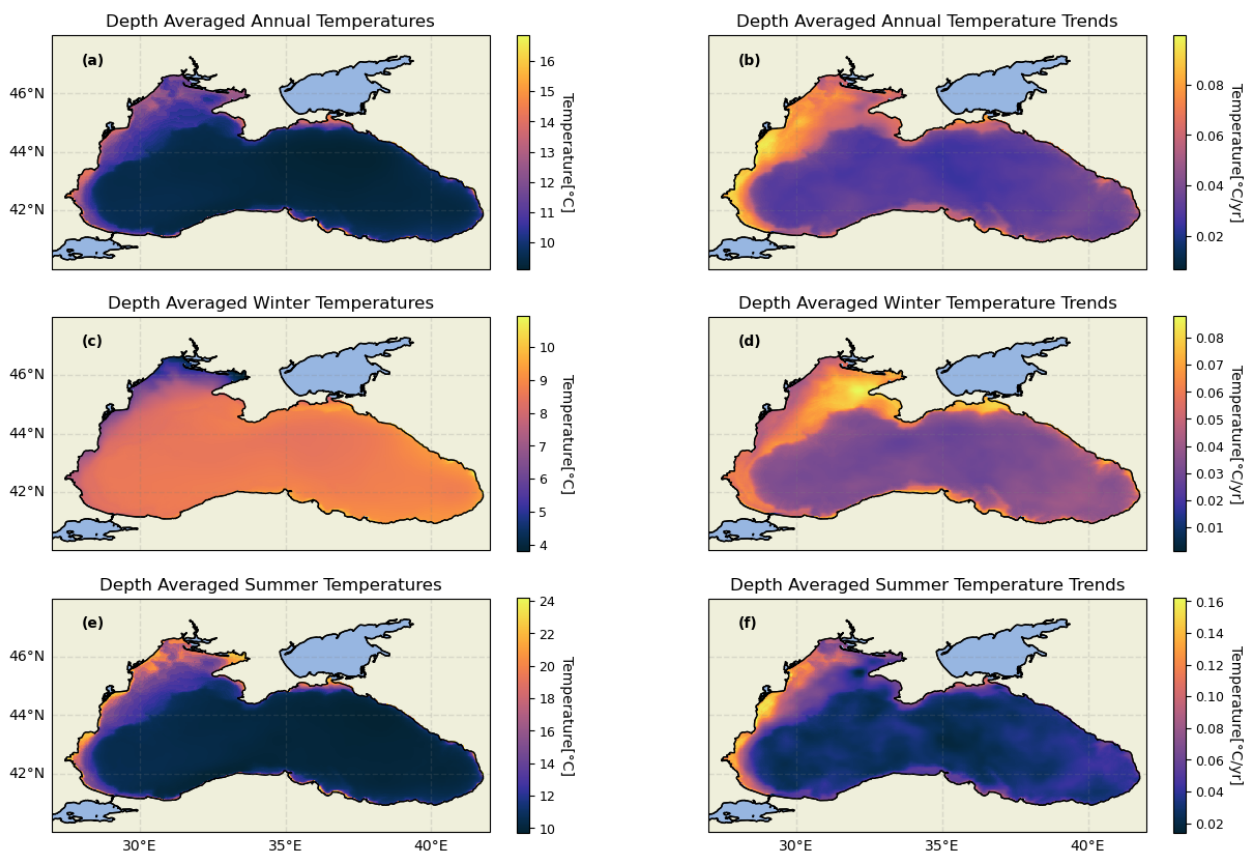
218

219   Figure 7: Depth averaged mean temperatures (**a**) annual, (**c**) winter, (**e**) summer; Depth averaged
220   linear trends (**b**) annual, (**d**) winter, (**f**) summer over the period January 1993 to December 2019.

221 For spatial analysis, depth-averaged annual temperatures and trends were used (Figure 7). Depth

222 averaged annual mean (Figure 7a) temperature varies between 9 and 17 C with the mean value of

223 9.893 ± 1.053 °C. Warm waters (> 11.999 °C) cover 6% of the Black sea and are located at

224 coastal areas as the depths of the coastal areas are lower than the other parts of the Black Sea.

225 Additionally, annual trends of coastal areas are higher than in the other parts of the Black Sea.

226 Under the influence of topography, trends are getting lower and lower from coastal areas to the

227 middle parts (Figure 7b). On the other hand, depth-averaged winter mean temperatures are

228 getting lower from west to east and from north to south (Figure 7c). Respectively, very cold

229 water can be seen ont the north-western shelf. 0.054% of the Black Sea is covered by cold water

230 (< 6.914 °C). Depth averaged annual mean temperatures vary between 3.5 and 11 °C in winter,

231 whereas, 9.5 and 24.5 °C in summer, which indicates having strong seasonality in temperatures

232 (Figure 7c, Figure 7e). Seasonality can be seen in the north-western shelf. In summer,

233 temperature values of 24 °C can be seen, whereas, temperature values of 3 °C can be seen in

234 winter. On the other hand, the middle parts are stable respectively, as there are the deep parts of

235 the Black Sea. Seasonality can be seen in depth-averaged temperature trends. In winter,

236 temperature trends vary between 0.04 and 1 °C; in contrast, temperature trends vary between 0.08

237 and 0.16 °C in summer in the north-western shelf (Figure 7d, Figure 7f). On the other hand, the

238 variability of deep parts is less than coastal parts.

239

240
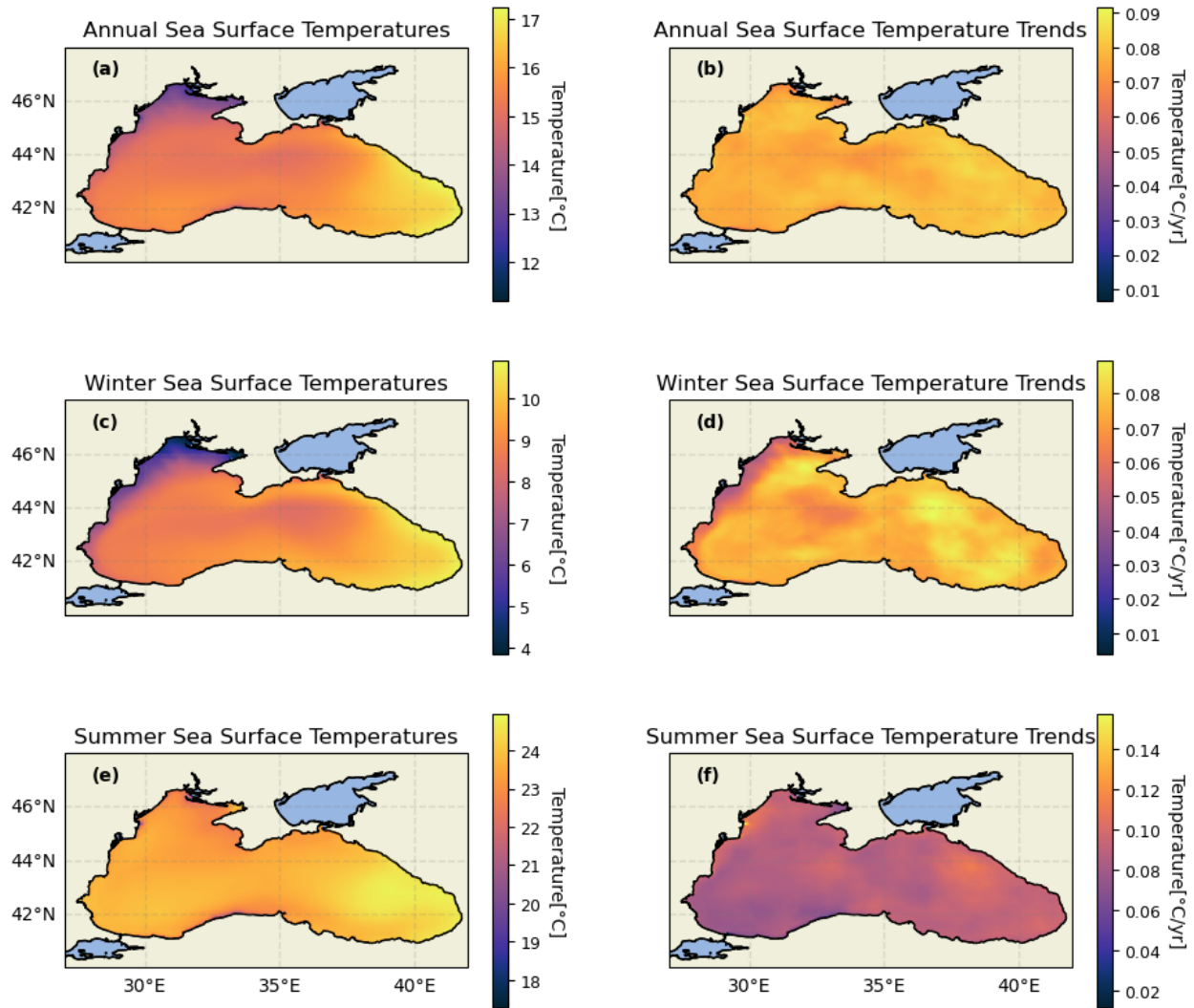
Figure 8: Mean SST (**a**) annual, (**c**) winter, (**e**) summer; SST linear trends (**b**) annual, (**d**) winter, (**f**) summer over the period January 1993 to December 2019.

Annual SST(ASST) and SST annual linear trends were observed (Figure 8). ASST range from 11 to 17.5 °C with the average value of 15.50 ± 0.74 °C (Figure 8a, Figure 8b). Cold waters (< 14.01 °C) are located at north-western shelf and cover 4.36% of Black Sea. ASST trends are generally higher than 0.08 °C and can reach up to 0.1 °C per year. However, there are seasonal differences in temperatures and temperature trends. Winter SST vary between 3.5 and 12 °C, whereas, Summer SST vary between 17 and 26 °C (Figure 8c, Figure 8e). Summer SST trends can reach up to 0.15 °C/season, while Winter SST trends reach only up to 0.09 °C/season (Figure

250 6d, Figure 6f). Main difference between winter and summer is at west coasts of north-western

251 shelf. Maximum increase in summer and minimum increase in winter are located at those areas.

4. Conclusion

253 In this study, changes in temperatures over 27 years periods are observed. The Black Sea

254 Physical Reanalysis system indicates a 0.036 °C/year increase in depth-averaged temperatures.

255 Minimum, maximum and mean temperatures have been increasing with a few exceptions, such as

256 in 2012 and 2017. However, particular importance was the investigation of different water

257 masses. An increase or decrease trend is not detected at intermediate and deep-water masses,

258 whereas, coastal and surface water masses have been warming by almost 0.01 °C per month. This

259 indicates that temperature changes are limited at upper-layer water masses. Another conclusion is

260 the warming of the CIL. The future of the CIL is still unknown and also the subject of research

261 (e.g. Stanev et al., 2019; Miladinova et al., 2018). We observed warming in CIL and temperatures

262 have reached 8 °C which is the maximum temperature for CIL. Hence, CIL characteristics may

263 be changing and should be investigated deeply.

264 Increasing trends can be seen all over the Black Sea. Not only SST but also depth-averaged

265 temperatures are increasing over 27 years period. Depth-averaged trends are higher in shelf areas

266 than deep areas , so deeper parts are not affected as much as shelf areas from climate change.

267 Variability of SST trends is low respectively. The north-western shelf has been warming faster

268 than the other parts of the Black Sea, especially in summer. Seasonal variability of the north-

269 western shelf is the highest in the Black Sea and also, western coasts of the Black Sea have been

270 warming faster in summer than in winter. This situation is noticeable in not only depth-averaged

271 temperature trends but also SST trends.

272 Salinity values along with the temperature were analyzed. In the case of salinity, the data between

273 CMEMS model data and Argo data is not correlated. In order to do an in depth analysis of the

274 salinity data for the sake of better understanding, the results of the salinity variations are not

275 included in this study. In addition, the salinity values do not show any significant

276 increase/decrease trend with time.

References

Benesty, J., Chen, J., Huang, Y., & Cohen, I. (2009). Pearson Correlation Coefficient. In: Noise Reduction in Speech Processing. In *Springer Topics in Signal Processing* (Vol. 2).

Bernstein, L., Bosch, P., Canziani, O., Chen, Z., Christ, R., Davidson, O., Hare, W., Huq, S., Karoly, D., Kattsov, V., Kundzewicz, Z., Liu, J., Lohmann, U., Manning, M., Matsuno, T., Menne, B., Metz, B., Mirza, M., Nicholls, N., Nurse, L., Palutikof, J., Parry, M., Qin, D., Ravindranath, N., Ren, J., Riahi, K., Rosenzweig, C., Rusticucci, M., Sokona, Y., Solomon, S., Stott, P., Stouffer, R., Swart, R., Tirpak, D., Vogel, C., Yohe, G., 2007. AR4 SYR Synthesis Report [WWW Document]. Synthesis (Stuttg).

Clark, P. U., Shakun, J. D., Marcott, S. A., Mix, A. C., Eby, M., Kulp, S., Levermann, A., Milne, G. A., Pfister, P. L., Santer, B. D., Schrag, D. P., Solomon, S., Stocker, T. F., Strauss, B. H., Weaver, A. J., Winkelmann, R., Archer, D., Bard, E., Goldner, A., … Plattner, G. K. (2016). Consequences of twenty-first-century policy for multi-millennial climate and sea-level change. *Nature Climate Change*, *6*(4), 360–369. https://doi.org/10.1038/nclimate2923

Dogan, M., & Ozgenc Aksoy, A. (2013). Investigation of the relation between meteorological parameters, North Atlantic Oscillation and groundwater levels in Torbali Region, Turkey. *Water and Environment Journal*, *27*(1). https://doi.org/10.1111/j.1747-6593.2012.00345.x

Esser, G., Kattge, J., & Sakalli, A. (2011). Feedback of carbon and nitrogen cycles enhances carbon sequestration in the terrestrial biosphere. *Global Change Biology*, *17*(2), 819–842. https://doi.org/10.1111/j.1365-2486.2010.02261.x

Ginzburg, A. I., Kostianoy, A. G., & Sheremet, N. A. (2004). Seasonal and interannual variability of the Black Sea surface temperature as revealed from satellite data (1982-2000). *Journal of Marine Systems*, *52*(1–4), 33–50. https://doi.org/10.1016/j.jmarsys.2004.05.002

Hirsch, R. M., & Slack, J. R. (1984). A Nonparametric Trend Test for Seasonal Data With Serial Dependence. *Water Resources Research*, *20*(6). https://doi.org/10.1029/WR020i006p00727

302   Hussain, M., & Mahmud, I. (2019). pyMannKendall: a python package for non parametric Mann

303   Kendall family of trend tests. *Journal of Open Source Software*, *4*(39), 1556.IPCC. (2014).

304   Climate Change 2014: Synthesis Report. Contribution of Working Groups I, II and III to the

305   Fifth Assessment Report of the Intergovernmental Panel on Climate Change. In *Ipcc*.

306   Ivanov V.A., Belokopytov V.N. (2015). Oceanography of the Black Sea. National Academy of

307   Sciences of Ukraine, Marine Hydrophysical Institute, Sevastopol, 210 p.

308   Jones, R. N. (2001). An environmental risk assessment/management framework for climate

309   change impact assessments. *Natural Hazards*, *23*(2–3).

310   https://doi.org/10.1023/A:1011148019213

311   Kazmin, A.S., Zatsepin, A.G., 2007. Long-term variability of surface temperature in the Black

312   Sea, and its connection with the large-scale atmospheric forcing. J. Mar. Syst. 68.

313   https://doi.org/10.1016/j.jmarsys.2007.01.002

314   Lima, L., Aydogdu, A., Escudier, R., Masina, S., Ciliberti, S. A., Azevedo, D., Peneva, E. L.,

315   Causio, S., Cipollone, A., Clementi, E., Cretí, S., Stefanizzi, L., Lecci, R., Palermo, F.,

316   Coppini, G., Pinardi, N., & Palazov, A. (2020). Black Sea Physical Reanalysis (CMEMS

317   BS-Currents) (Version 1) set. Copernicus Monitoring Environment Marine Service

318   (CMEMS). https://doi.org/10.25423/CMCC/BLKSEA_MULTIYEAR_PHY_007_004

319   Mee, L. D., Friedrich, J., & Gomoiu, M. T. (2005). Restoring the Black Sea in times of

320   uncertainty. *Oceanography*, *18*(SPL.ISS.2). https://doi.org/10.5670/oceanog.2005.45

321   Miladinova, S., Stips, A., Garcia-Gorriz, E., & Macias Moy, D. (2018). Formation and changes

322   of the Black Sea cold intermediate layer. *Progress in Oceanography*, *167*.

323   https://doi.org/10.1016/j.pocean.2018.07.002

324   Mohamed, B., Ibrahim, O., & Nagy, H. (2022). Sea Surface Temperature Variability and Marine

325   Heatwaves in the Black Sea. *Remote Sensing*, *14*(10), 2383.

326 Oguz, T., Dippner, J. W., & Kaymaz, Z. (2006). Climatic regulation of the Black Sea hydro-
327   meteorological and ecological properties at interannual-to-decadal time scales. *Journal of*
328   *Marine Systems*, *60*(3–4). https://doi.org/10.1016/j.jmarsys.2005.11.011

329 Özsoy, E., & Ünlüata, Ü. (1997). Oceanography of the Black Sea: A review of some recent
330   results. In *Earth-Science Reviews* (Vol. 42, Issue 4). https://doi.org/10.1016/S0012-
331   8252(97)81859-4

332 Patz, J. A., Campbell-Lendrum, D., Holloway, T., & Foley, J. A. (2005). Impact of regional
333   climate change on human health. In *Nature* (Vol. 438, Issue 7066).
334   https://doi.org/10.1038/nature04188

335 Rhein, M., Rintoul, S. R., Aoki, S., Campos, E., Chambers, D., Feely, R. A., Gulev, S., Johnson,
336   G. C., Josey, S. A., Kostianoy, A., Mauritzen, C., Roemmich, D., Talley, L. D., & Wang, F.
337   (2014). Observations: Ocean. In: Climate Change 2013: The Physical Science Basis.
338   Contribution of Working Group I to the Fifth Assessment Report of the Intergovernmental
339   Panel on Climate Change. In *Cambridge University Press, Cambridge, United Kingdom and*
340   *New York, NY, USA. 255* (Vol. 13, Issue 4).

341 Sakalli, A., & Başusta, N. (2018). Sea surface temperature change in the Black Sea under climate
342   change: A simulation of the sea surface temperature up to 2100. *International Journal of*
343   *Climatology*, *38*(13), 4687–4698. https://doi.org/10.1002/joc.5688

344 Shapiro, G. I., Aleynik, D. L., & Mee, L. D. (2010). Long term trends in the sea surface
345   temperature of the Black Sea. *Ocean Science*, *6*(2). https://doi.org/10.5194/os-6-491-2010

346 Stanev, E. V., & Peneva, E. L. (2001). Regional sea level response to global climatic change:
347   Black Sea examples. *Global and Planetary Change*, *32*(1). https://doi.org/10.1016/S0921-
348   8181(01)00148-5

349 Stanev, E. V., Peneva, E., & Chtirkova, B. (2019). Climate Change and Regional Ocean Water
350   Mass Disappearance: Case of the Black Sea. *Journal of Geophysical Research: Oceans*,
351   *124*(7). https://doi.org/10.1029/2019JC015076

352   Stewart, K., Kassakian, S., Krynytzky, M., Dijulio, D., & Murray, J. W. (2007). Oxic, suboxic,

353   and anoxic conditions in the Black Sea. In *The Black Sea Flood Question: Changes in*

354   *Coastline, Climate, and Human Settlement*. https://doi.org/10.1007/978-1-4020-5302-3_1

355   Thenmozhi, M. & Kottiswaran, S.V. (2016). Analysis of Rainfall Trend Using Mann– Kendall

356   Test and the Sen'S Slope Estimator in Udumalpet of Tirupur District in Tamil Nadu.

357   *International Journal of Agricultural Science and Research (IJASR)*, *6*(2).

358   Wong, A. P., Wijffels, S. E., Riser, S. C., Pouliquen, S., Hosoda, S., Roemmich, D., ... & Park, H.

359   M. (2020). Argo data 1999–2019: two million temperature-salinity profiles and subsurface

360   velocity observations from a global array of profiling floats. *Frontiers in Marine Science*,

361   700.